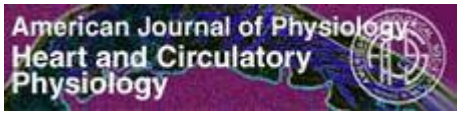

Atrioventricular Plane Displacement is the Major Contributor to Left Ventricular Pumping in Healthy Adults, Athletes and Patients with Dilated Cardiomyopathy

Journal:	*AJP: Heart and Circulatory Physiology*
Manuscript ID:	H-01148-2006.R1
Manuscript Type:	Original Article
Date Submitted by the Author:	n/a
Complete List of Authors:	Carlsson, Marcus; Clinical Physiology Ugander, Martin; Clinical Physiology Mosen, Henrik; Clinical Physiology Buhre, Torsten; Dep of Sport Sciences Arheden, Håkan; Clinical Physiology
Key Words:	Left Ventricle, Stroke Volume, Cardiac Pumping, MRI

Atrioventricular Plane Displacement is the Major Contributor to Left Ventricular Pumping in Healthy Adults, Athletes and Patients with Dilated Cardiomyopathy

Marcus Carlsson[1], Martin Ugander[1], Henrik Mosén[1], Torsten Buhre[2], Hakan Arheden[1].

Department of Clinical Physiology (1) Lund University Hospital, Sweden

Department of Sport Sciences (2), Malmo University, Sweden

Running head: AV-plane Displacement is the Major Contributor to LV Pumping

Corresponding author: Hakan Arheden, MD, PhD, Assoc. Prof.
Department of Clinical Physiology,
Lund University Hospital,
Lund, SE-22185 Sweden
Tel +46 46 173328; Fax: +46 46 151769
E-Mail: hakan.arheden@med.lu.se

ABSTRACT

Background: Previous studies using echocardiography in healthy subjects have reported conflicting data regarding the percentage of the stroke volume (SV) of the left ventricle (LV) resulting from longitudinal and radial function, respectively. Therefore, the aim was to quantify the percentage of SV explained by longitudinal atrioventricular plane displacement (AVPD) in controls, athletes and patients with decreased LV function due to dilated cardiomyopathy (DCM). **Methods and Results:** Twelve healthy subjects, twelve elite triathletes and twelve patients with DCM and ejection fraction below 30% were examined by cine magnetic resonance imaging. AVPD and SV were measured in long- and short-axis images, respectively. The percentage of the SV explained by longitudinal function ($SV_{AVPD\%}$) was calculated as the mean epicardial area of the largest short-axis slices in end-diastole multiplied by the AVPD and divided by the SV. SV was higher in athletes (mean±SEM, 140±4 ml, p=0.009) and lower in patients (72±7 ml, p<0.001) compared to controls (116±6 ml). AVPD was similar in athletes (17±1 mm, p=0.45) and lower in patients (7±1 mm, p<0.001) compared to controls (16±0 mm). $SV_{AVPD\%}$ was similar both in athletes (57±2 %, p=0.51) and in patients (67±4 %, p=0.24) compared to controls (60±2%). **Conclusions:** Longitudinal AVPD is the primary contributor to LV pumping and accounts for ~60% of the SV. Although AVPD is less than half in patients with DCM compared to controls and athletes, the contribution of AVPD to LV function is maintained, which can be explained by the larger short-axis area in DCM.

Key words: left ventricle, stroke volume, cardiac pumping, MRI

INTRODUCTION

Cardiac pumping is the result of the contraction of myocardial fibers organized in different orientations and different layers (15, 35), resulting in both longitudinal and radial shortening of the ventricles (27). Longitudinal shortening through atrioventricular plane displacement (AVPD) can be observed as the movement of the base of the ventricles towards the apex in systole (16, 21, 25, 29). Previous studies using echocardiography in healthy subjects have reported conflicting data regarding the percentage of the left ventricular stroke volume (SV) resulting from AVPD, although this could be explained by differences in methodology and definitions (4, 9, 43). Furthermore, the percentage of the SV explained by AVPD may differ between controls, athletes and patients with decreased cardiac function, and this could be of importance in understanding differences in the pumping physiology between these groups.

It has been proposed that the portion of the SV which is generated by AVPD (SV_{AVPD}) can be derived by multiplying the AVPD by the epicardial left ventricular area located 2-3 cm apical to the base of the heart (25). This method has been employed using echocardiography in a study of healthy volunteers (9). However, the method does not take into account the variation in diameter of the left ventricle within the range of the AVPD, and has not been validated by independent measurements. Magnetic resonance imaging (MRI) gives the opportunity to measure both endocardial and epicardial volumes with great accuracy and precision, and to image the whole heart in any plane. This makes it possible to validate the derived method against direct volumetry of the stroke volume generated by AVPD.

Therefore, the purposes of this study were a) to measure the percentage of the SV explained by longitudinal function measured as AVPD in healthy subjects, athletes and patients with severely decreased left ventricular function due to dilated cardiomyopathy (DCM) using

MRI, b) to revise the method for calculation of the longitudinal component of the stroke volume (SV_{AVPD}) , c) to validate the revised method against direct volumetry of the SV generated by the AVPD and finally, d) to anatomically localize where the stroke volume is generated.

MATERIALS AND METHODS

Study population

The study was approved by the local ethics committee. Written informed consent was either obtained (controls, athletes and 9 patients) or waived by the ethics committee (3 patients). Twelve healthy controls (mean age 24 years, 5 women), twelve elite triathletes (mean age 35 years, 4 women) and twelve patients with dilated cardiomyopathy (DCM) and ejection fraction below 30 % (mean age 54 years, 4 women) were examined with magnetic resonance imaging (MRI) in the supine position. The controls had normal blood pressure (<140/90 mmHg), a normal electrocardiogram (ECG), no medical history of any cardiac condition and no cardiovascular medication. The triathletes were selected from the Swedish national elite of triathletes, and exercised 12±3 hours/week (mean±SD). The subjects in the patient group were selected from patients with idiopathic DCM referred for a routine clinical MRI. DCM was determined by medical records, MRI findings and the exclusion of significant coronary disease by myocardial perfusion imaging and/or coronary angiography.

Magnetic Resonance Imaging

A 1.5 T MRI scanner (Philips Intera CV, Philips, Best, the Netherlands) with a cardiac synergy coil was used. Cine images in the short-axis plane and three long-axis planes; the two-chamber, four-chamber and left ventricular outflow tract views were obtained in all subjects during end-expiratory apnea.

Sequences and imaging parameters

A steady-state free precession sequence with retrospective ECG triggering was used to achieve 30 time phases per heart cycle giving a temporal resolution of typically 30 ms, repetition time 2.8 ms, echo time 1.4 ms, flip angle 60^0 and spatial resolution of 1.4x1.4x8 mm. Parallel imaging with a SENSE factor of 2 was used in the short-axis images. Fifty phases per heart cycle were acquired in the long axis planes in the control group. In nine control subjects, a radial stack of 18 long-axis slices of the left ventricle (LV) was obtained at 10 degree intervals (Fig. 1) (8).

Image analysis

All images were evaluated using freely available software (Segment 1.466 http://segment.heiberg.se) (18).

Stroke volume

The stroke volume (SV) was calculated from manual delineations of short-axis images by subtracting the systolic from the diastolic ventricular volume as previously described (30). This can be expressed as the following formula:

$$SV = Endo_{ED} - Endo_{ES} \quad \text{(Equation 1)}$$

where $Endo_{ED}$ and $Endo_{ES}$ are the endocardial contours of the left ventricle in end diastole and end systole, respectively. Moreover, it is known that the epicardial volume of the LV (Epi_{ED} or Epi_{ES}) is equal to the endocardial volume plus the myocardial volume according to the following formulae.

$$Epi_{ED} = Endo_{ED} + \text{Myocardial volume}_{ED} \quad \text{(Equation 2)}$$

$$Epi_{ES} = Endo_{ES} + Myocardial\ volume_{ES} \quad \text{(Equation 3)}$$

Furthermore, it is know that the myocardial volume is constant over the cardiac cycle (17, 36, 40), and thus:

$$Myocardial\ volume_{ES} = Myocardial\ volume_{ES} \quad \text{(Equation 4)}$$

Hence, equations 1, 2, 3 and 4 can be combined and rewritten as the following.

$$SV = Epi_{ED} - Epi_{ES} = Endo_{ED} - Endo_{ES} \quad \text{(Equation 5)}$$

Consequently, the stroke volume was calculated using both the epicardial and endocardial borders of the LV. The radius of each short axis slice was calculated as the square root of the ratio between the area and π (3.14). The difference in radius from end diastole to end systole was calculated and the mean of the apical and midventricular two thirds of the left ventricle was obtained for each subject.

Derived method for SV_{AVPD}

The atrioventricular plane displacement (AVPD) can be seen as a piston-like movement of the AV-plane in the base-apex direction within the LV. The volume explained by the AVPD is the volume at the base of the LV between the position of the AV-plane in end diastole and end systole (Fig. 2A-D). The SV generated by the AVPD (SV_{AVPD}) was calculated as the left ventricular short-axis area multiplied by the AVPD. The basal part of the ventricle including the AV-plane is not flat, but rather shaped like a dome. This is both illustrated schematically and seen *in vivo* in Fig. 2. This dome shape has consequences for the derived method to calculate the part of the SV generated by the longitudinal AVPD. The area multiplied

by the AVPD cannot be the short-axis area at the mitral annulus (d_2), but rather must be the largest epicardial short-axis area of the LV (d_1). It is important to note that the area used to calculate the longitudinal contribution to the SV should be the epicardial area as explained in Fig. 2C and D. The epicardial area was taken from the short-axis slice or slices which encompassed the range of the AVPD. Thus, for patients, the area of the single largest short-axis slice was used because the thickness of one short-axis slice and the mean AVPD were both 8 mm. In controls and athletes the mean AVPD was 16 mm and therefore the mean area of the largest two slices was used for these groups. The resulting volume was divided by the SV to calculate the percentage of SV explained by longitudinal function for the LV ($SV_{AVPD\%}$). Furthermore, the diameter at the mitral annulus (d_2) and the epicardial short-axis at the midventricular level (d_1) were measured in the four-chamber MR images of the control subjects in order to compare the diameter used for SV_{AVPD} (d_1) and mitral annular excursion volume (d_2) (4).

Validation of SV_{AVPD} *by the volumetric method*

In nine control subjects the volume contribution of the AVPD to the stroke volume was evaluated in a stack of radial long axis slices by direct planimetry (Fig. 1). For each long-axis slice in a radial stack, the epicardial border of the LV in end diastole was outlined. Next, the position of the AV-plane in end systole was identified. The outline of the epicardial border of the LV in end diastole was then translated along the long-axis of the LV towards the apex so that the basal part of the outline had a position corresponding to the position of the AV-plane in end systole. The volume difference between the two borders in the base of the end diastolic contour was calculated for all radial slices.

Atrioventricular plane displacement

The AVPD was measured in long axis images (Fig. 3). The basal location of the muscular insertion of the ventricle to the AV-plane was manually identified in each of the three long-axis images along a line parallel to the long axis of the LV. This resulted in six locations for measuring the AV-plane position in the LV. The maximum AVPD was calculated from end diastole to end systole and the average of the six locations was calculated.

Anatomical location of the contribution to the stroke volume

The difference in epicardial volume between end diastole and end systole for each short-axis slice was calculated for all subjects. The relative contribution of each short-axis slice position to the stroke volume was calculated by dividing the difference in epicardial volume by the total stroke volume for that subject. Furthermore, the contribution to stroke volume for each individual short-axis slice was compared to the epicardial volume of that slice in end diastole.

Apex position

In nine control subjects the most apical part of the ventricle was determined in end diastole and end systole in all radial slices, and the mean distance of the apical motion was measured. In all other subjects, the position of the LV apex in end diastole and end systole was determined in the three long-axis slices and the distance between the positions was measured.

Statistical analysis

Measurements of volumes and distances are expressed as mean ± standard error of the mean (SEM) and the range. The Mann-Whitney test was used to test the significance of the differences between variables. A p-value <0.05 was defined as statistically significant. The relationship between variables was determined by Pearson's correlation coefficient. Bias

(difference between two methods) was expressed as mean±SD of the differences between the two measures.

RESULTS

Study population

Subject characteristics are listed in Table 1. Athletes and patients were older than controls but there was no difference in body surface area. Heart rate and LV volumes were higher in patients compared to controls. Athletes had slightly higher end diastolic volumes compared to controls. Typical MR-images from a control, athlete and patient are shown in Fig 4.

Validation of SV_{AVPD}

The SV_{AVPD} determined by the volumetric method did not differ from the SV_{AVPD} from the derived method in the nine control subjects (70±14 ml vs. 68±11 ml, p=0.67). The regression line comparing the volumetric and derived method (r=0.82, p=0.007) was described by the following equation:

derived≡(1.1•volumetric)-3.0

The difference between the volumetric and the derived method was 2±8 ml.

Stroke volume

The SV was higher in athletes (140±4 ml, range 115–157, p=0.009) and lower in patients (72±7 ml, range 43–121, p<0.001) compared to controls (116±6 ml, range 77–152), Fig. 5. The SV indexed to body surface area was also higher in athletes (74±2 ml/m², range 65–83, p<0.001), and lower in patients (36±3 ml/m², range 21–61, p<0.001) compared to controls (60±2 ml/m², range 48–73). There was a linear relation between SV determined by epicardial

delineation (SV_{epi}) and endocardial delineation (SV_{endo}) ($r = 0.99$, $p<0.001$) according to the equation:

$$SV_{endo} = (1.0 \bullet SV_{epi}) - 1.4$$

Also, the difference between SV_{epi} and SV_{endo} was 0.8±5.4 ml.

Atrioventricular plane displacement

AVPD for controls was 16±0 mm (range 14 – 19). AVPD was similar in athletes (17±1 mm, range 14–20, $p=0.45$) and lower in patients (7±1 mm, range 5–11, $p<0.001$), Fig 5.

Derived method $SV_{AVPD\%}$

$SV_{AVPD\%}$ for controls was 60±2 % (range 51-69). $SV_{AVPD\%}$ did not differ for athletes (57±2 %, range 41-66, $p=0.51$) or for patients (67±4 %, range 49-88, $p=0.24$), Fig. 5.

Short-axis area

The short-axis areas used for calculating the SV_{AVPD} were 42±2 cm^2 (range 30-53) for controls. The athletes' areas were similar (48±2 cm^2, range 38-58, $p=0.08$) but the patients' areas were larger (67±4 cm^2, range 45-83, $p<0.001$). In controls, the epicardium moved 3.4±0.2 mm (range 1.8-4.5) towards the center of the LV from end diastole to end systole in the apical and midventricular two-thirds of the LV. The epicardial radial inward motion for athletes did not differ (3.7±0.2 mm, range 2.6-5.0, $p = 0.51$) compared to controls, but the epicardial motion of the patients was lower (1.0±0.2 mm, range -0.3-2.3, $p<0.001$). For controls, the epicardial short-axis diameter at the midventricular level (d_1, 70±2 mm, range 62-81 mm) was nearly double the diameter of the mitral annulus (d_2, 36±2, range 28-48 mm).

Anatomical location of contribution to SV

The relative contribution to stroke volume was plotted for each short-axis slice position of the LV for each group (Fig. 6). The greatest portion of the stroke volume was generated in slice positions at the base of the LV. Only a weak correlation was found between the relative contribution to stroke volume of each short-axis slice and the relative size of that slice ($r=0.35$, $p<0.001$). Regardless, the largest difference in epicardial volume and thus contribution to stroke volume was found at the base of the ventricles in all groups (Fig. 6). The location of the largest part of the SV at the base of the ventricle can be seen in the superimposed contours of the long axis images in Fig 4.

Apical motion

The apical motion between end diastole and end systole was 1.9±0.5 mm (range -0.1-5.1), 1.8±0.5 mm (range -0.8-5.3) and 0.1±0.2 mm (range -1.4-1.4) for controls, athletes and patients, respectively. Athletes and controls were similar ($p=0.93$) but patients had less apical movement than controls ($p=0.004$). Negative apical movement, i.e. apical dyskinesia, was seen in seven patients (see example in Fig 4) but only in one healthy subject.

DISCUSSION

The major finding of this study was that ~60% of the stroke volume is generated by the longitudinal AVPD and this does not differ in athletes or in patients with dilated ventricles. The largest portion of the stroke volume can be found at the base of the ventricles. Furthermore, the previously proposed method for calculating the SV generated by AVPD (25) has been revised and validated. The revised method showed good agreement to direct planimetry of this volume.

Longitudinal function

AVPD has been recognized as an important contributor to LV pumping (13, 16, 19, 22, 25) and used as a measure of global LV function (1, 2, 37), but the magnitude of the longitudinal contribution to SV has been unclear (4, 5, 9, 43). The current study showing that 60% of the SV is derived from AVPD ($SV_{AVPD\%}$) differs from earlier studies using echocardiography suggesting the $SV_{AVPD\%}$ to be as high as 82 % (9) and from the volume generated by the mitral annular movement which has been reported to be 19% (4). The discrepancy compared to the first study may be explained by known methodological limitations with two dimensional echocardiography, for example an underestimation of measured volumes as discussed by the authors of that study (9). MRI has the advantage of accurate and precise volume measurements due to three-dimensional coverage of the whole LV. Furthermore, MRI offers excellent soft tissue contrast which gives the ability to delineate the epicardium and endocardium, thereby making MRI particularly well suited for these types of studies. In the current study, short-axis images were positioned parallel to the AV-plane and thus perpendicular to the AVPD, giving optimal accuracy in measurement of the short-axis area. Furthermore, the current study has taken into account the variation in diameter of the left ventricle and used the mean of the short axis areas encompassed by the range of the AVPD. This revised method showed good agreement

compared to direct measurement of the SV_{AVPD}. The second study using three dimensional transesophageal echocardiography determined the part of the stroke volume explained by mitral annular excursion to be 19 % (4). However, as shown by the current study, the mitral annular excursion volume does not represent the entire portion of the stroke volume generated by AVPD. This can be explained by the finding that the diameter of the mitral annulus was half of the diameter of the midventricular part of the ventricle. This has been commented by those authors in a recent reply (5) to a letter to the editor (43) in this journal. In Figure 2C, the mitral annular excursion volume would be represented by the area at d_2 multiplied by AVPD, whereas the entire SV_{AVPD} measured in the present study is defined as the area at d_1 multiplied by AVPD. AVPD was greater in the present study (16 mm) compared with the study by Carlhall and coworkers (10 mm), and this can be explained by several factors. Firstly, the subjects in Carlhall´s study were older (56±11 years) and AVPD is known to decrease with age (42). Secondly, six of the subjects of Carlhall´s study were imaged during general anaesthesia and this could affect AVPD as commented by Carlhall and coworkers. Lastly, the AVPD was measured at the mitral annulus in Carlhall´s study and at the tip of the muscular wall in our study. Noteably, the AVPD of the present study is in accordance with recently published normal values of AVPD by MRI (26).

Radial function

Since sixty percent of the SV is generated by longitudinal AVPD, the remaining forty percent of the SV must be the result of radial shortening. The endocardial movement towards the center of the lumen has previously been described as radial thickening due to the contraction of circular myocardial fibers (31, 35), but has been shown to be the result of more complex myocardial mechanics (3, 12, 17, 28, 36). The current study has shown that either epicardial or endocardial contours can be used interchangeably for the calculation of LV stroke

volume. This is in line with earlier findings of a constant volume of the LV myocardium despite shortening and thickening during myocardial contraction (17, 36, 40). Thus, the current results show that inward motion of the endocardium is primarily the result of longitudinal shortening and redistribution of myocardium, as has been suggested previously (25, 40), Fig. 2. Furthermore, the epicardial area at the mitral annulus in end diastole is smaller than the mid-ventricular area because of the dome shape of the basal part of the LV. The dome shape will contribute to an apparent inward epicardial motion at the base of the LV during AVPD. Isolated radial function can be identified in the radial inward movement of the epicardium in the midventricular and apical two-thirds of the LV. This movement was found to be 3-4 mm in controls and athletes, and approximately 1 mm in patients. The movement in controls is slightly larger but in agreement with previous studies of the findings in previous studies in humans (approximately 2 mm) (9, 25) and dogs (approximately 1.5 mm) (36).

The reported contribution of longitudinal function to the inward motion of the endocardium has implications for the measurement of radial contribution to LV function. The reduction of endocardial diameter during systole, also called fractional shortening (11), has been used as a measure of radial function (31). Fractional shortening, however, is influenced by longitudinal function as shown in the current study, and thus not solely a product of radial function. Therefore, it may be motivated to re-evaluate the role of fractional shortening as a measure of radial function. The inward motion of the epicardium described in the present study corresponds in part to the “crescent effect” of the LV described by Kovacs and coworkers (32, 44). The “crescent effect” is the radial pericardial displacement of the LV most often seen at the postero-lateral wall. However, as seen in Fig. 2 and 4 we found an inward epicardial movement circumferentially in the short-axis plane. Thus, the “crescent effect” in part corresponds to the radial function of the LV.

Methodological aspects of using epicardial areas

The rationale for using epicardial areas when determining longitudinal function can be explained by considering the left ventricle as the tube of a telescope which can shorten and lengthen along its long-axis. The volume of the telescope decreases when the tube shortens and this would be the stroke volume of the tube. In order to calculate the decrease in volume, two measures need to be known. 1) The decreased length of the tube (the AV-plane displacement of the LV), and, 2) the outer cross sectional area of the tube (the short axis epicardial area). The outer area of the tube would be used because the decrease in volume is not affected by what is inside the tube. The volume decrease is only affected by what has disappeared from where the tube was before it was shortened lengthwise. Two tubes with the same outer area but one with a thick wall and the other with a thin wall (different thickness of the myocardium in the LV) will decrease the same volume given the same outer area and same long axis shortening. Also, the wall of the tube is non-compressible, i.e. it retains its volume when shortening the tube. This analogy is true for the myocardium, the volume will be the same during the cardiac cycle because its non-compressible nature.

Apical movement

The present study found that the contribution to the SV by apical motion is negligible (Fig. 6) and that the apex remains essentially stationary during systole. Earlier studies have also reported the apex to be relatively stationary (3, 14, 20, 34, 38). We (6) and others (44) have previously reported a limited shortening (0.9±0.5% and 0.03±1.0% respectively) of the entire heart in the apex-base direction during systole, and a limited movement (2.3±0.2 mm) of the center of volume of the heart during the cardiac cycle (7). Taken together, these findings

imply that the apical movement can be no more than a few millimetres, and this is confirmed by the present study. In contrast, a study using epicardially implanted radiopaque markers in sheep reported that apical motion constitutes 22% of the longitudinal shortening of the ventricle (33). However, the same study found that isolated AVPD correlated better to ventricular stroke work than AVPD combined with apex movement. This implies that apical epicardial motion is not a large contributor to the SV. Furthermore, it is possible that the increased apical movement found in the sheep study may be an effect of the surgical preparation with pericardiotomy. Moreover, the epicardial contour of the apex moves very little but this does not imply that the apical myocardium does not contribute to LV pumping. The mechanics of the myocardium as such were not studied in the present study.

Similarity of $SV_{AVPD\%}$ *between the groups*

Controls, athletes and patients had similar $SV_{AVPD\%}$. This can be explained by the non-significant trend towards larger short-axis areas in athletes, and significantly larger short-axis areas in patients compared to controls. This is further discussed in Fig. 6.

Anatomical location of stroke volume

The largest part of the stroke volume is generated at the base of the ventricles in all groups (Fig 6). In patients, the most basal short axis image was particularly prominent, although the difference compared to the healthy groups was not significant. This is explained by a large basal area and lower AVPD, typically 7 mm. With 8 mm slice thickness, the position of the base of the ventricle in patients will shift one short-axis slice position during systole, thus generating a large amount of the stroke volume. Furthermore, the SV is decreased in the patient group which gives a larger percentage of the contribution of the most basal slice to the SV compared to the

healthy groups. In controls and athletes, the position of the base of the ventricle will shift two short-axis slice positions during systole (AVPD of 16 mm and slice thickness of 8 mm). The area is smaller in the most basal slice compared to the slice below it. This explains why the second slice generates the most SV in the healthy groups.

The fact that the stroke volume is primarily generated in the basal part of the left ventricle has implications for cardiac imaging. The basal location of a large part of the SV underscores the importance of imaging the entire LV including the base. Furthermore, great care must be taken to account for the AVPD when measuring the SV by planimetry.

Further studies

Heart rate and level of physical exertion may affect SV_{AVPD} and studies undertaken in situations with increased cardiac output would be of value. Also, it would be of interest to investigate patients with coronary artery disease, left ventricular hypertrophy and mitral valve disease since the relationship between longitudinal and radial function in these patients has been reported to differ from healthy subjects (24).

Limitations

AVPD is known to decrease with age (42), and in the present study patients were older and had higher heart rates than controls. Thus, part of the difference in AVPD may be related to these disparities. Three of the patients had atrial fibrillation, which has been reported to decrease the AVPD (10). The patients with atrial fibrillation, however, had a $SV_{AVPD\%}$ and AVPD which was similar to the other patients, suggesting that this may not be a major factor in DCM. The contraction of the myocardial tissue as such is more complex than solely longitudinal and radial shortening. The coupling between longitudinal, helical and circumferential myocardial

fibers (3, 41), and the torsion of the myocardium during contraction (23, 35, 39) have not been studied. However, the aim of the study was not to investigate the mechanics of myocardial fibers as such. Furthermore, this study did not seek to investigate differences in efficiency of the contraction caused by the differences in ventricular geometry between the groups. However, future studies are merited to elucidate such differences.

In conclusion, the present study has demonstrated that the largest part of the stroke volume is generated at the base of the ventricles and that longitudinal atrioventricular plane displacement is the primary contributor to LV pumping, accounting for ~60 % of the left ventricular stroke volume. Although AVPD is less than half in patients with DCM compared to controls and athletes, the contribution of AVPD to LV function is maintained. This can be explained by the larger short-axis area in patients with DCM.

Acknowledgements:

This study has been funded in part by grants from the Swedish Research Council, the Swedish Heart and Lung Foundation, Lund University Faculty of Medicine and the Region of Scania.

Disclosures: None.

REFERENCES

1. **Alam M, Hoglund C, Thorstrand C, and Philip A.** Atrioventricular plane displacement in severe congestive heart failure following dilated cardiomyopathy or myocardial infarction. *J Intern Med* 228: 569-575, 1990.

2. **Alam M and Rosenhamer G.** Atrioventricular plane displacement and left ventricular function. *J Am Soc Echocardiogr* 5: 427-433, 1992.

3. **Buckberg GD, Mahajan A, Jung B, Markl M, Hennig J, and Ballester-Rodes M.** MRI myocardial motion and fiber tracking: a confirmation of knowledge from different imaging modalities. *Eur J Cardiothorac Surg* 29 Suppl 1: S165-177, 2006.

4. **Carlhall C, Wigstrom L, Heiberg E, Karlsson M, Bolger AF, and Nylander E.** Contribution of mitral annular excursion and shape dynamics to total left ventricular volume change. *Am J Physiol Heart Circ Physiol* 287: H1836-1841, 2004.

5. **Carlhall C, Wigstrom L, Heiberg E, Karlsson M, Bolger AF, and Nylander E.** REPLY 10.1152/ajpheart.00618.2006. *Am J Physiol Heart Circ Physiol* 291: H2551-2552, 2006.

6. **Carlsson M, Cain P, Holmqvist C, Stahlberg F, Lundback S, and Arheden H.** Total heart volume variation throughout the cardiac cycle in man. *Am J Physiol Heart Circ Physiol* 287: H243-250, 2004.

7. **Carlsson M, Rosengren A, Ugander M, Ekelund U, Cain PA, and Arheden H.** Center of volume and total heart volume variation in healthy subjects and patients before and after coronary bypass surgery. *Clin Physiol Funct Imaging* 25: 226-233, 2005.

8. **Clay S, Alfakih K, Radjenovic A, Jones T, Ridgway JP, and Sinvananthan MU.** Normal range of human left ventricular volumes and mass using steady state free precession MRI in the radial long axis orientation. *Magma* 19: 41-45, 2006.

9. **Emilsson K, Brudin L, and Wandt B.** The mode of left ventricular pumping: is there an outer contour change in addition to the atrioventricular plane displacement? *Clin Physiol* 21: 437-446, 2001.

10. **Emilsson K and Wandt B.** The relation between mitral annulus motion and left ventricular ejection fraction in atrial fibrillation. *Clin Physiol* 20: 44-49, 2000.

11. **Feigenbaum H.** Echocardiographic evaluation of cardiac chambers. In: *Echocardiography* (5:th ed.). Philadelphia: Lea& Feibger, 1994, p. 134-180.

12. **Gallagher KP, Osakada G, Matsuzaki M, Miller M, Kemper WS, and Ross J, Jr.** Nonuniformity of inner and outer systolic wall thickening in conscious dogs. *Am J Physiol* 249: H241-248, 1985.

13. **Gauer OH.** Volume Changes of the Left Ventricle During Blood Pooling and Exercise in the Intact Animal - Their Effects on Left Ventricular Performance. *Physiol Rev* 35: 143-155, 1955.

14. **Gorman JH, 3rd, Gupta KB, Streicher JT, Gorman RC, Jackson BM, Ratcliffe MB, Bogen DK, and Edmunds LH, Jr.** Dynamic three-dimensional imaging of the mitral valve and left ventricle by rapid sonomicrometry array localization. *J Thorac Cardiovasc Surg* 112: 712-726, 1996.

15. **Greenbaum RA and Gibson DG.** Regional non-uniformity of left ventricular wall movement in man. *Br Heart J* 45: 29-34, 1981.

16. **Hamilton WF and Rompf JH.** Movement of the base of the ventricle and the relative constancy of the cardiac volume. *Am J Physiol* 102: 559-565, 1932.

17. **Hartley CJ, Latson LA, Michael LH, Seidel CL, Lewis RM, and Entman ML.** Doppler measurement of myocardial thickening with a single epicardial transducer. *Am J Physiol* 245: H1066-1072, 1983.

18. **Heiberg E, Wigström L, Carlsson M, Bolger AF, and Karlsson M.** Time Resolved Three-dimensional Automated Segmentation of the Left Ventricle. *In Proceedings of IEEE Computers in Cardiology* 32: 599-602, 2005.

19. **Henein MY and Gibson DG.** Long axis function in disease. *Heart* 81: 229-231, 1999.

20. **Hoffman EA and Ritman EL.** Invariant total heart volume in the intact thorax. *Am J Physiol* 249: H883-890, 1985.

21. **Holmgren BS.** The movement of the mitro-aortic ring recorded simultaneosly by cineroentgenography and electrocardiography. *Acta Radiologica* 27: 171-176, 1946.

22. **Ingels NB, Jr.** Myocardial fiber architecture and left ventricular function. *Technol Health Care* 5: 45-52, 1997.

23. **Ingels NB, Jr., Hansen DE, Daughters GT, 2nd, Stinson EB, Alderman EL, and Miller DC.** Relation between longitudinal, circumferential, and oblique shortening and torsional deformation in the left ventricle of the transplanted human heart. *Circ Res* 64: 915-927, 1989.

24. **Jones CJ, Raposo L, and Gibson DG.** Functional importance of the long axis dynamics of the human left ventricle. *Br Heart J* 63: 215-220, 1990.

25. **Lundback S.** Cardiac Pumping and Function of the Ventricular Septum. *Acta Physiol Scand* 127: 8-101, 1986.

26. **Maceira AM, Prasad SM, Khan M, and Pennell DJ.** Normalized Left Ventricular Systolic and Diastolic Function by Steady State Free Precession Cardiovascular Magnetic Resonance. *Journal of Cardiovascular Magnetic Resonance* 8: 417-426, 2006.

27. **McDonald IG.** The shape and movements of the human left ventricle during systole. A study by cineangiography and by cineradiography of epicardial markers. *Am J Cardiol* 26: 221-230, 1970.

28. **Myers JH, Stirling MC, Choy M, Buda AJ, and Gallagher KP.** Direct measurement of inner and outer wall thickening dynamics with epicardial echocardiography. *Circulation* 74: 164-172, 1986.

29. **Odqvist H.** A roentgen cinematographic study of the movements of the mitral ring during heart action. *Acta Radiologica* 26: 392-396, 1945.

30. **Pennell DJ.** Ventricular volume and mass by CMR. *J Cardiovasc Magn Reson* 4: 507-513, 2002.

31. **Popovic ZB, Sun JP, Yamada H, Drinko J, Mauer K, Greenberg NL, Cheng Y, Moravec CS, Penn MS, Mazgalev TN, and Thomas JD.** Differences in left ventricular long-axis function from mice to humans follow allometric scaling to ventricular size. *J Physiol* 568: 255-265, 2005.

32. **Riordan MM and Kovacs SJ.** Relationship of pulmonary vein flow to left ventricular short-axis epicardial displacement in diastole: model-based prediction with in vivo validation. *Am J Physiol Heart Circ Physiol* 291: H1210-1215, 2006.

33. **Rodriguez F, Tibayan FA, Glasson JR, Liang D, Daughters GT, Ingels NB, Jr., and Miller DC.** Fixed-apex mitral annular descent correlates better with left ventricular systolic function than does free-apex left ventricular long-axis shortening. *J Am Soc Echocardiogr* 17: 101-107, 2004.

34. **Rogers WJ, Jr., Shapiro EP, Weiss JL, Buchalter MB, Rademakers FE, Weisfeldt ML, and Zerhouni EA.** Quantification of and correction for left ventricular systolic long-axis

shortening by magnetic resonance tissue tagging and slice isolation. *Circulation* 84: 721-731, 1991.

35. **Rushmer RF, Crystal DK, and Wagner C.** The functional anatomy of ventricular contraction. *Circ Res* 1: 162-170, 1953.

36. **Sabbah HN, Marzilli M, and Stein PD.** The relative role of subendocardium and subepicardium in left ventricular mechanics. *Am J Physiol* 240: H920-926, 1981.

37. **Simonson JS and Schiller NB.** Descent of the base of the left ventricle: an echocardiographic index of left ventricular function. *J Am Soc Echocardiogr* 2: 25-35, 1989.

38. **Slager CJ, Hooghoudt TE, Serruys PW, Schuurbiers JC, Reiber JH, Meester GT, Verdouw PD, and Hugenholtz PG.** Quantitative assessment of regional left ventricular motion using endocardial landmarks. *J Am Coll Cardiol* 7: 317-326, 1986.

39. **Streeter DD, Jr., Spotnitz HM, Patel DP, Ross J, Jr., and Sonnenblick EH.** Fiber orientation in the canine left ventricle during diastole and systole. *Circ Res* 24: 339-347, 1969.

40. **Sundblad P and Wranne B.** Influence of posture on left ventricular long- and short-axis shortening. *Am J Physiol Heart Circ Physiol* 283: H1302-1306, 2002.

41. **Torrent-Guasp F, Ballester M, Buckberg GD, Carreras F, Flotats A, Carrio I, Ferreira A, Samuels LE, and Narula J.** Spatial orientation of the ventricular muscle band: physiologic contribution and surgical implications. *J Thorac Cardiovasc Surg* 122: 389-392, 2001.

42. **Wandt B, Bojo L, and Wranne B.** Influence of body size and age on mitral ring motion. *Clin Physiol* 17: 635-646, 1997.

43. **Wandt B, Brodin LA, and Lundback S.** Misinterpretation About the Contribution of the Left Ventricular Long-Axis Shortening to the Stroke Volume 10.1152/ajpheart.00530.2006. *Am J Physiol Heart Circ Physiol* 291: H2550-, 2006.

44. **Waters EA, Bowman AW, and Kovacs SJ.** MRI-determined left ventricular "crescent effect": a consequence of the slight deviation of contents of the pericardial sack from the constant-volume state. *Am J Physiol Heart Circ Physiol* 288: H848-853, 2005.

LEGENDS

Table 1. Subjects characteristics. Data for continuous variables are presented as mean±SEM. BSA = body surface area, LVEDV = left ventricular end diastolic volume, LVESV = left ventricular end systolic volume, LVEF = left ventricular ejection fraction, LBBB = left bundle branch block, ACEI = angiotensin converting enzyme inhibitor, ARB = angiotensin II receptor blocker, ß-blocker = beta blocker, NYHA-class = symptoms of heart failure according to the New York Heart Association classification, * $p<0.05$, *** $p<0.001$ denotes significance differences from controls for continuous variables.

Figure 1. Radial projections of the left ventricle. A. A short-axis MR image of the LV in end diastole. White lines indicate how the radial stack of 18 long axis slices was acquired at 10° intervals. The dashed white line shows the position of the long-axis images in **B** and **C**. The solid white line in **B** shows the contour of the epicardium in end diastole. The contour is copied to the end systolic image (**C**). The curved dotted line is the contour of the basal part of the LV in end diastole moved to the position of the AV-plane in end systole. The volume illustrated by diagonal lines between the contours represents the stroke volume generated by the AVPD. The white arrow indicates concomitant radial shortening causing a further decrease in area of the basal part of the left ventricle during systole.

Figure 2. Schematic illustration of left ventricular pumping and corresponding *in vivo* MR images.

A. The epicardial contour of a schematic LV with only longitudinal pumping is shown in a long-axis view. The atrioventricular plane displacement (AVPD, vertical arrows) of the LV can be viewed as a piston-like movement of the basal part of the ventricle. The valves are omitted from

the illustration for the sake of simplicity. The broken lines indicate the position of the atrioventricular plane (AV-plane) in end systole. The volume of blood ejected from the heart by the AVPD is the volume basal to the position of the AV-plane in end systole, shown in grey.

B. d_1 denotes the largest diameter of the LV defined as the greatest epicardial area in a short axis plane. d_2 denotes the diameter at the position of the mitral valve. The grey region indicates the diameter (d_1) multiplied by the AVPD. This region is the same size as the grey region in A, see D below.

C. Myocardium is added to the model, thereby reducing the inner contour (endocardium) of the ventricle. The myocardium in end diastole is indicated by solid lines and in end systole by dashed lines. The volume of the myocardium is constant throughout the cardiac cycle. The myocardium is rearranged as it pulls the AV-plane towards the apex and therefore appears thickened. The portion of the stroke volume which is generated by the AVPD is again indicated in grey and is identical to the grey regions in panels A and B. This illustrates that the area at d_1 (the largest short axis diameter) shall be used when calculating the contribution of AVPD to stroke volume. The stroke volume caused by the AVPD would be underestimated if the area of either the mitral annulus at d_2 or the endocardial area at d_3 would be used.

D. The grey region in A and C is divided by a dotted line and broken apart. When adding them together, the grey region in B is generated. This illustrates why the largest epicardial area of the ventricle should be multiplied by the AVPD in the derived method for calculating SV_{AVPD}.

E. A schematic short-axis view in end diastole (solid line) and end systole (broken line) at the level of the thin dotted line in C. The horizontal dashed lines indicate the position of the non-moving epicardium in end diastole and end systole. Note that in this model there is no radial sqeezing motion. However, the endocardium will still move inwards during systole (compare Fig.

2F) as the result of the longitudinal AVPD, and this gives the false impression of a squeezing motion when viewing the endocardium in a short-axis plane.

F. The left ventricle in four-chamber long-axis MR images (panels 1 and 2) and corresponding short-axis images at the levels indicated by thin dotted lines (panels 3-6). The left ventricle (LV), right ventricle (RV), left atrium (LA) and right atrium (RA) can be seen. The solid white line is the contour of the epicardium in end diastole. The end-diastolic epicardial contour is copied to end systole. The curved dotted line in panels 1 and 2 is the basal contour of the epicardium in end diastole moved to the position of the AV-plane in end systole. The area between these contours (arrows) corresponds to the grey region in A-D. The piston-like movement of a smaller basal part of the ventricle into a larger midventricular part as seen in panels 1 and 2 explains most of the apparent epicardial movement inwards during systole seen in panels 3 and 4. In contrast, the epicardial area from the level of panels 5 and 6 becomes smaller as the position approaches the apex. Thus, longitudinal AVPD will not move a smaller area into a larger area in the apical and midventricular parts of the ventricle, meaning that the epicardial inward movement at these levels rather reflects true radial function.

Figure 3. Measurement of atrioventricular plane displacement (AVPD).

MR images of a control subject in end diastole and end systole in the two-chamber (2ch), left ventricular outflow tract (LVOT) and four-chamber (4ch) long-axis planes and a short-axis plane (SA). The lines in the short-axis image illustrate the position in which the long-axis planes were obtained. The dotted vertical lines denote the long-axis of the LV, perpendicular to the AV-plane, along which the AVPD was measured. The horizontal dotted lines indicate the position of the AV-plane in end diastole and end systole in the anterior wall (2ch), inferolateral wall (LVOT)

and anterolateral wall (4ch), respectively. The solid vertical lines in the end systolic images show the AVPD at each location of measurement.

Figure 4. Illustration of representative regional differences in left ventricular volume changes. MR images in the two-chamber (2ch), left ventricular outflow tract (LVOT) and four-chamber (4ch) long-axis views in a control subject (left panel), an athlete (middle panel) and a patient (right panel) in end diastole (ED) and end systole (ES). The epicardial contours of the left ventricles are indicated by solid lines in end diastole and broken lines in end systole. The epicardial delineations shown are superimposed to the right of the corresponding long axis images. The difference between the volumes of the epicardium in ED and ES is the stroke volume, since the volume of the myocardium does not change during myocardial contraction. The greater part of the difference in area between the ED and ES contour in the superimposed contours can be seen at the base of the LV in all subjects. However, there is also an area difference at the midventricular and apical part of the ventricle. These differences illustrate the portions of the SV attributed to radial shortening. Note the dyskinesia of the apical parts in the four-chamber view in the patient.

Figure 5. (A) Atrioventricular plane displacement (AVPD), **(B)** left ventricular stroke volume (SV) and **(C)** contribution of longitudinal AVPD to the stroke volume ($SV_{AVPD\%}$) for controls, athletes and patients. Solid circles denote mean and error bars denote SEM, ** $p<0.01$, *** $p<0.001$, ns $p>0.05$ versus controls.

Figure 6. Anatomic location of the change in left ventricular volume, i.e. contribution to stroke volume. The difference in epicardial volume for each short-axis slice between end

diastole and end systole was calculated and the relative contribution of each short-axis slice to the stroke volume was calculated for all subjects. The mean for controls, athletes and patients respectively is shown on the vertical axis as % contribution to SV. Error bars indicate SEM. The horizontal axis indicates the short axis position of the left ventricle in end diastole where base is the level of the AV-plane in end diastole.

Table 1. Subjects characteristics

	Controls	Athletes	Patients
Number, n	12	12	12
Age, years	24±1	35±1***	54±2***
Females, n (%)	5 (42)	4 (33)	4 (33)
BSA, m^2	1.94±0.03	1.90±0.03	2.03±0.04
Sinus rhythm, n (%)	12 (100)	12 (100)	9 (67)
Atrial fibrillation, n (%)	0 (100)	0 (100)	3 (33)
Heart rate, beats/min	63±2	55±1	77±2 *
LVEDV, ml	185±10	218±10 *	333±27 ***
LVESV, ml	69±5	78±7	261±24 ***
LVEF, %	63±1	65±2	22±2 ***
LBBB, n (%)	-	-	4 (33)
Medication, n (%)	0 (0)	0 (0)	12 (100)
ACEI	-	-	11 (92)
ARB	-	-	2 (17)
ß-blocker	-	-	11 (92)
Diuretics	-	-	9 (75)
Digoxin	-	-	9 (75)
NYHA class	-	-	2.4±0.1
Cause of DCM, n (%)			
Myocarditis	-	-	1 (8)
Adriamycin	-	-	1 (8)
Unknown	-	-	10 (83)

Data for continuous variables are presented as mean±SEM. BSA = body surface area, LVEDV = left ventricular end diastolic volume, LVESV = left ventricular end systolic volume, LVEF = left ventricular ejection fraction, LBBB = left bundle branch block, ACEI = angiotensin converting

enzyme inhibitor, ARB = angiotensin II receptor blocker, ß-blocker = beta blocker, NYHA-class = symptoms of heart failure according to the New York Heart Association classification, * $p<0.05$, *** $p<0.001$ denotes significance differences from controls for continuous variables.

FIGURES

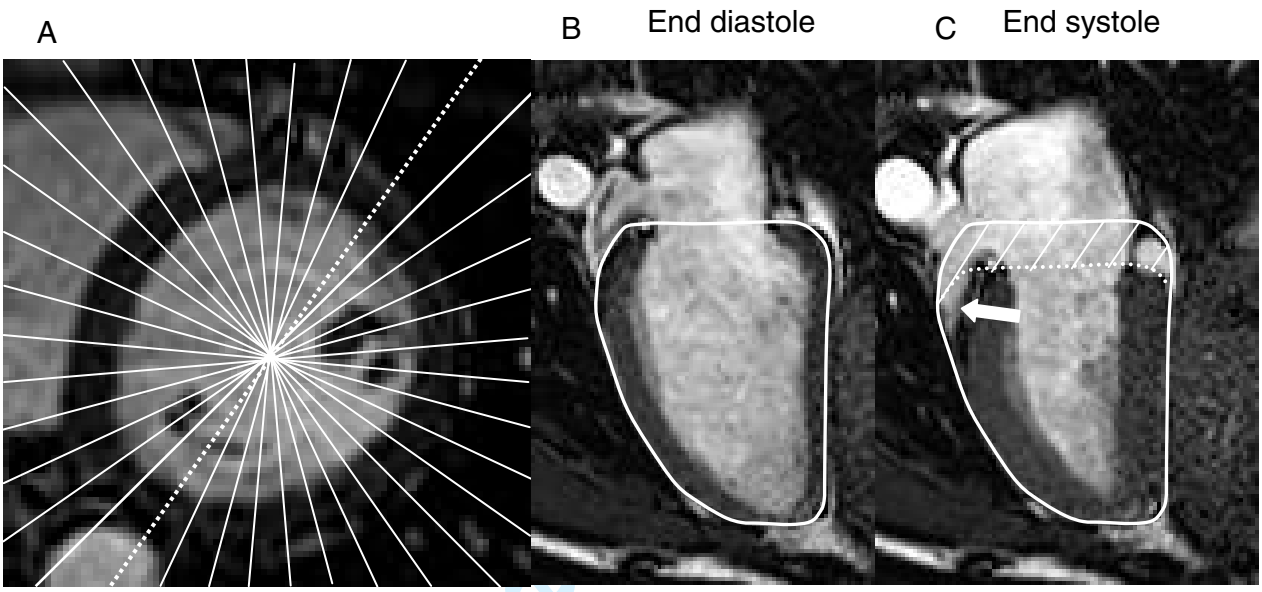

Figure 1. Radial projections of the left ventricle. A. A short-axis MR image of the LV in end diastole. White lines indicate how the radial stack of 18 long axis slices was acquired at 10° intervals. The dashed white line shows the position of the long-axis images in **B** and **C**. The solid white line in **B** shows the contour of the epicardium in end diastole. The contour is copied to the end systolic image (**C**). The curved dotted line is the contour of the basal part of the LV in end diastole moved to the position of the AV-plane in end systole. The volume illustrated by diagonal lines between the contours represents the stroke volume generated by the AVPD. The white arrow indicates concomitant radial shortening causing a further decrease in area of the basal part of the left ventricle during systole.

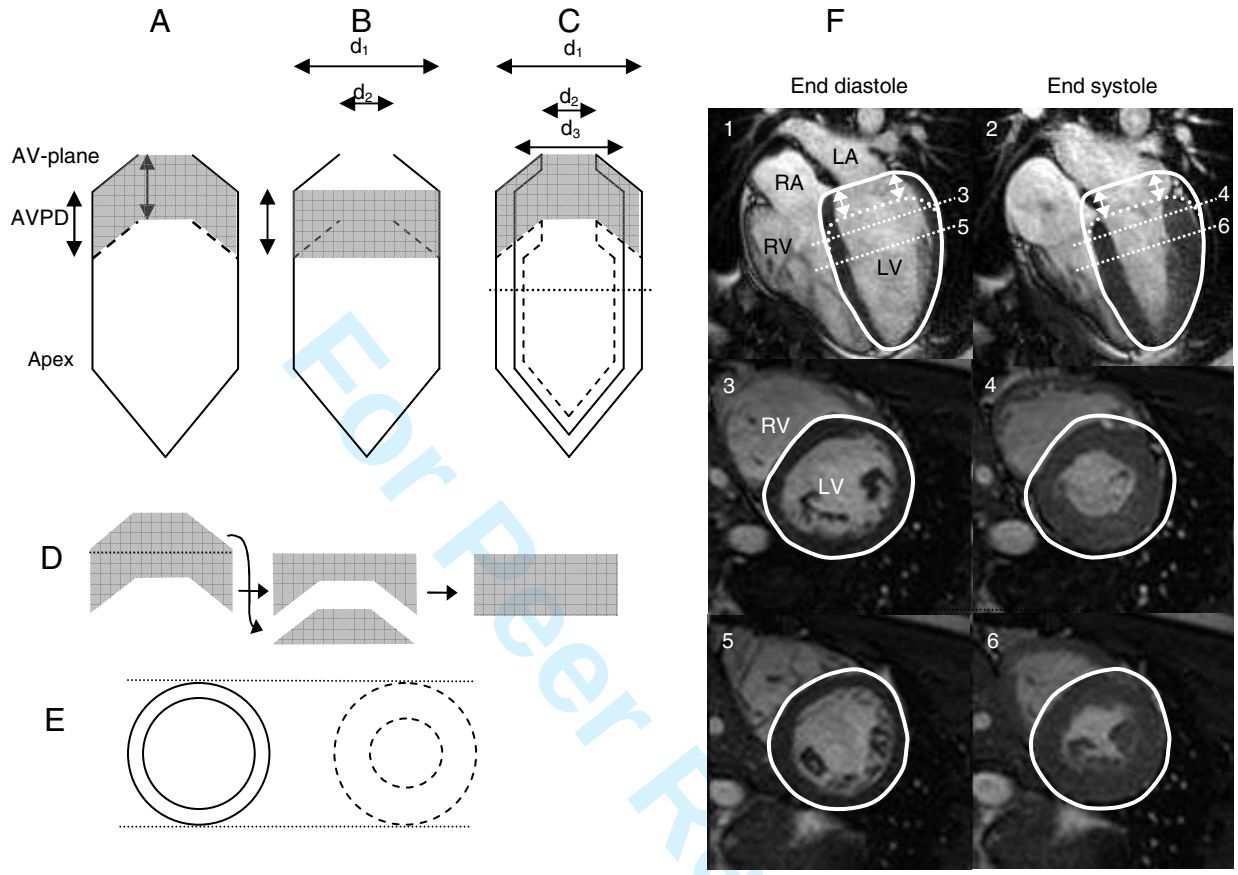

Figure 2. Schematic illustration of left ventricular pumping and corresponding *in vivo* MR images.

A. The epicardial contour of a schematic LV with only longitudinal pumping is shown in a long-axis view. The atrioventricular plane displacement (AVPD, vertical arrows) of the LV can be viewed as a piston-like movement of the basal part of the ventricle. The valves are omitted from the illustration for the sake of simplicity. The broken lines indicate the position of the

atrioventricular plane (AV-plane) in end systole. The volume of blood ejected from the heart by the AVPD is the volume basal to the position of the AV-plane in end systole, shown in grey.

B. d_1 denotes the largest diameter of the LV defined as the greatest epicardial area in a short axis plane. d_2 denotes the diameter at the position of the mitral valve. The grey region indicates the diameter (d_1) multiplied by the AVPD. This region is the same size as the grey region in A, see D below.

C. Myocardium is added to the model, thereby reducing the inner contour (endocardium) of the ventricle. The myocardium in end diastole is indicated by solid lines and in end systole by dashed lines. The volume of the myocardium is constant throughout the cardiac cycle. The myocardium is rearranged as it pulls the AV-plane towards the apex and therefore appears thickened. The portion of the stroke volume which is generated by the AVPD is again indicated in grey and is identical to the grey regions in panels A and B. This illustrates that the area at d_1 (the largest short axis diameter) shall be used when calculating the contribution of AVPD to stroke volume. The stroke volume caused by the AVPD would be underestimated if the area of either the mitral annulus at d_2 or the endocardial area at d_3 would be used.

D. The grey region in A and C is divided by a dotted line and broken apart. When adding them together, the grey region in B is generated. This illustrates why the largest epicardial area of the ventricle should be multiplied by the AVPD in the derived method for calculating SV_{AVPD}.

E. A schematic short-axis view in end diastole (solid line) and end systole (broken line) at the level of the thin dotted line in C. The horizontal dashed lines indicate the position of the non-moving epicardium in end diastole and end systole. Note that in this model there is no radial sqeezing motion. However, the endocardium will still move inwards during systole (compare Fig. 2F) as the result of the longitudinal AVPD, and this gives the false impression of a squeezing motion when viewing the endocardium in a short-axis plane.

F. The left ventricle in four-chamber long-axis MR images (panels 1 and 2) and corresponding short-axis images at the levels indicated by thin dotted lines (panels 3-6). The left ventricle (LV), right ventricle (RV), left atrium (LA) and right atrium (RA) can be seen. The solid white line is the contour of the epicardium in end diastole. The end-diastolic epicardial contour is copied to end systole. The curved dotted line in panels 1 and 2 is the basal contour of the epicardium in end diastole moved to the position of the AV-plane in end systole. The area between these contours (arrows) corresponds to the grey region in A-D. The piston-like movement of a smaller basal part of the ventricle into a larger midventricular part as seen in panels 1 and 2 explains most of the apparent epicardial movement inwards during systole seen in panels 3 and 4. In contrast, the epicardial area from the level of panels 5 and 6 becomes smaller as the position approaches the apex. Thus, longitudinal AVPD will not move a smaller area into a larger area in the apical and midventricular parts of the ventricle, meaning that the epicardial inward movement at these levels rather reflects true radial function.

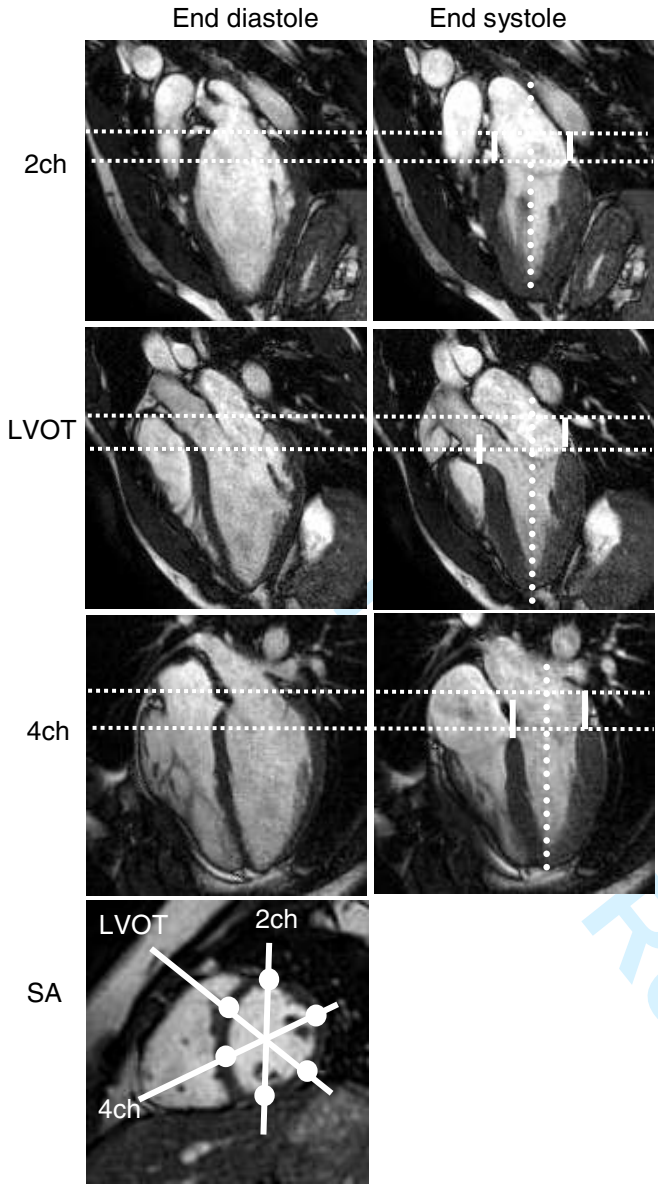

Figure 3. Measurement of atrioventricular plane displacement (AVPD).

MR images of a control subject in end diastole and end systole in the two-chamber (2ch), left ventricular outflow tract (LVOT) and four-chamber (4ch) long-axis planes and a short-axis plane (SA). The lines in the short-axis image illustrate the position in which the long-axis planes were obtained. The dotted vertical lines denote the long-axis of the LV, perpendicular to the AV-plane, along which the AVPD was measured. The horizontal dotted lines indicate the position of the AV-plane in end diastole and end systole in the anterior wall (2ch), inferolateral wall (LVOT)

and anterolateral wall (4ch), respectively. The solid vertical lines in the end systolic images show the AVPD at each location of measurement.

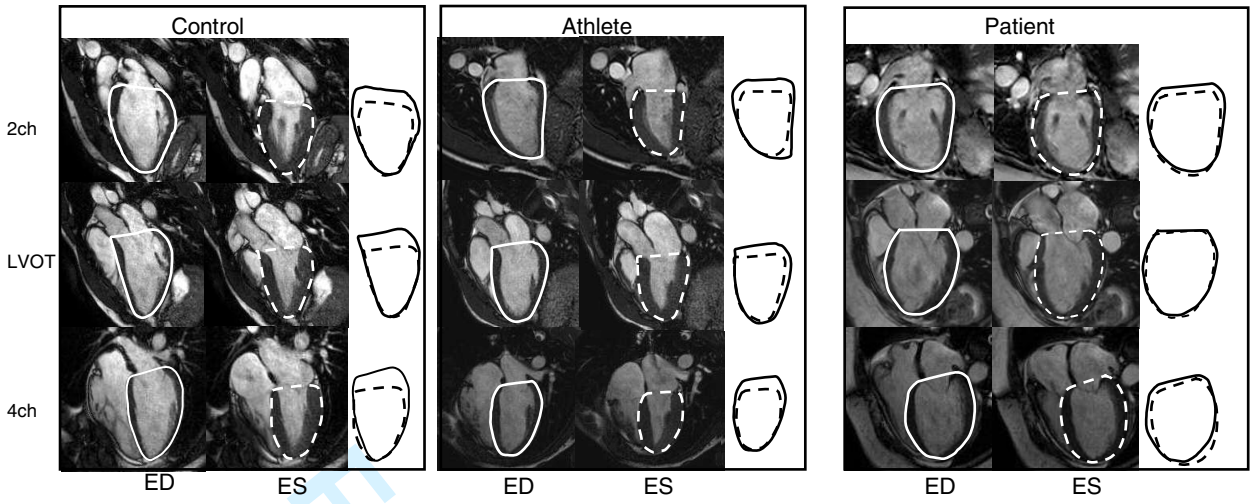

Figure 4. Illustration of representative regional differences in left ventricular volume changes. MR images in the two-chamber (2ch), left ventricular outflow tract (LVOT) and four-chamber (4ch) long-axis views in a control subject (left panel), an athlete (middle panel) and a patient (right panel) in end diastole (ED) and end systole (ES). The epicardial contours of the left ventricles are indicated by solid lines in end diastole and broken lines in end systole. The epicardial delineations shown are superimposed to the right of the corresponding long axis images. The difference between the volumes of the epicardium in ED and ES is the stroke volume, since the volume of the myocardium does not change during myocardial contraction. The greater part of the difference in area between the ED and ES contour in the superimposed contours can be seen at the base of the LV in all subjects. However, there is also an area difference at the midventricular and apical part of the ventricle. These differences illustrate the portions of the SV attributed to radial shortening. Note the dyskinesia of the apical parts in the four-chamber view in the patient.

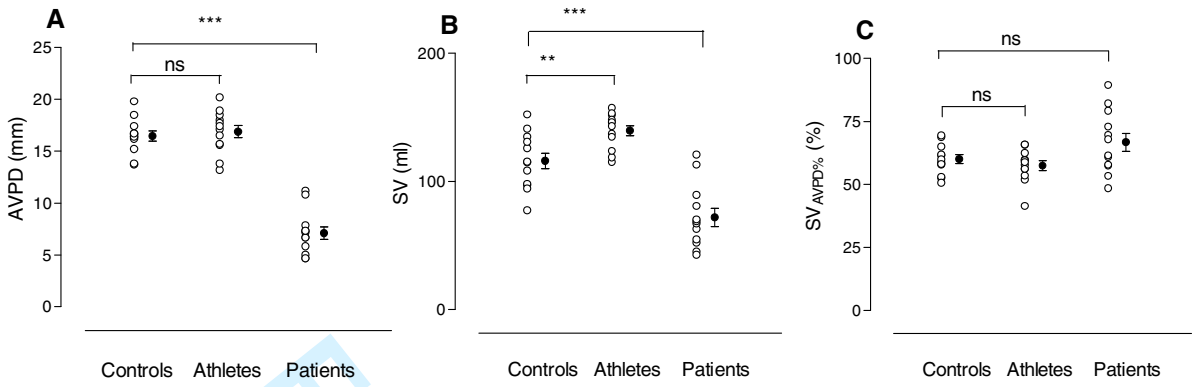

Figure 5. **(A)** Atrioventricular plane displacement (AVPD), **(B)** left ventricular stroke volume (SV) and **(C)** contribution of longitudinal AVPD to the stroke volume ($SV_{AVPD\%}$) for controls, athletes and patients. Solid circles denote mean and error bars denote SEM, ** $p<0.01$, *** $p<0.001$, ns $p>0.05$ versus controls.

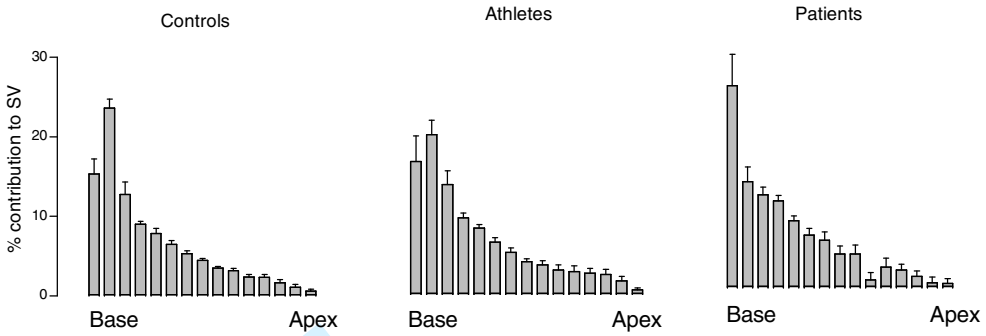

Figure 6. Anatomic location of the change in left ventricular volume, i.e. contribution to stroke volume. The difference in epicardial volume for each short-axis slice between end diastole and end systole was calculated and the relative contribution of each short-axis slice to the stroke volume was calculated for all subjects. The mean for controls, athletes and patients respectively is shown on the vertical axis as % contribution to SV. Error bars indicate SEM. The horizontal axis indicates the short axis position of the left ventricle in end diastole where base is the level of the AV-plane in end diastole.